Angewandte Communications

Zigzag Ribbon

DOI: 10.1002/anie.201((will be filled in by the editorial staff))

Synthesis of Nitrogen Doped ZigZag-Edge Peripheries: Dibenzo-*9a*-azaphenalene as Repeating Unit**

Reinhard Berger, Angelos Giannakopoulos, Prince Ravat, Manfred Wagner, David Beljonne, Xinliang Feng,* Klaus Müllen**

***Abstract**: A bottom-up approach toward stable and monodisperse segments of graphenes with a nitrogen doped zigzag-edge is introduced. Exemplified by the so far unprecedented dibenzo-9a-azaphenalene (DBAPhen) as core unit, a versatile synthetic concept is proposed targeting larger nitrogen doped zigzag-nanographenes and graphene nanoribbons.*

Phenalene (**1**) is the prototype of a non-Kekulé polycyclic aromatic hydrocarbon (PAH).[1] It can occur as neutral, delocalized radical with 13 π-electrons, as an anionic (14 π-e$^-$) or as an cationic (12 π-e$^-$) aromatic compound.[2] Being the smallest D_{3h}-symmetric PAH next to benzene, it is a structural motif for graphene having full-zigzag edge peripheries. Repetition of this motif can lead to nanographenes or graphene nanoribbons (GNRs) with full-zigzag edge.[3] In contrast to the fully benzenoid nanographenes or GNRs,[4] segments of graphene with zigzag peripheries have unpaired electrons primarily located on the edges.[5] These zigzag graphenes are candidates for spintronics.[6] However, they are kinetically unstable regarding oxidation or dimerization,[1b, 7] and the synthesis of larger monodisperse, open-shell zigzag-graphene-segments remains a challenging task as so-called "synthetic organic spin chemistry".[8]

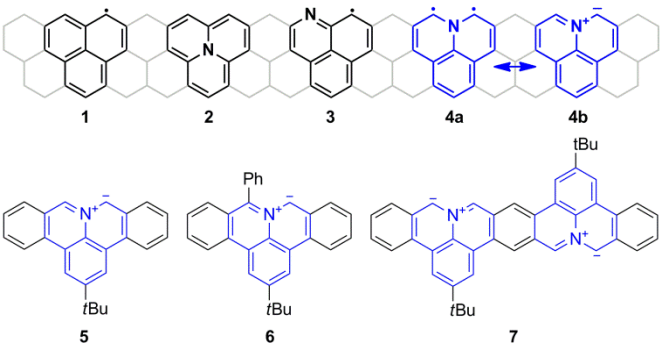

Figure 1. Phenalene **1** and aza-derivatives **2** - **4**; dibenzoazaphenalenes **5** - **6** and their repeated structural motif in dimer **7**.

Here, we introduce the synthesis of 9*a*-azaphenalenes with dibenzo-elongated zigzag-edge (**5** - **6**) and propose a protocol for the solution-based bottom-up approach towards doped zigzag-GNRs. This is exemplified on the next higher homolog **7**, an aza-derivative of dibenzoheptazethrene synthesized by Clar et al.[9] In contrast to previously studied aza-phenalenes, such as 9*b*-azaphenalene (cyclazine) (**2**),[10] and 1-azaphenalene (**3**),[11] the introduction of nitrogen into the zigzag edge results in a neutral diradical **4a**. The latter can, in principle, be stabilized in a zwitterionic valence bond structure of an azomethine ylide (AMY) type **4b.**[12] The high chemical reactivity of 9*a*-aza "doping" is demonstrated by dimerization and the [2+3]-cycloaddition reaction of in-situ created *t*Bu-DBAPhen **5**. Single crystal analysis revealed the selective addition of dimethyl acetylenedicarboxylate (DMAD) to the AMY side of **5**. Steric shielding of the highly reactive periphery in **5** with bulky aryl group was achieved in **6** to inhibit self-dimerisation and increase the kinetic stability.

The synthesis of **5** – **6**, was accomplished by base treatment of corresponding precursor derivatives 2-(*tert*-butyl)-8H-isoquinolino[4,3,2-de]phenanthridin-9-ium chloride (**11**), 2-(*tert*-butyl)-8-phenyl-8*H*-isoquinolino[4,3,2-de]phenanthridin-9-ium tetrafluoroborate (**12**). These precursors can all be derived from 2,6-dibromo-4-(*tert*-butyl)aniline (**8**) (Scheme 1). The synthetic protocol of the precursor comprises the following steps: First, Suzuki coupling was performed between **8** and 1-hydroxy-3*H*-2,1-benzoxaborole (**9**), to afford **10** or **13** followed by repeated Suzuki coupling of **13** and l,5-dibora-2,6-dioxa-*sym*-hydrindacene-l,5-diol (**14**)[13] in the case of **15**. Second, HCl-induced microwave assisted, cyclization of **10** and **15** affords precursors **11** and **16**, while further Grignard addition and hydride abstraction of **11** provide **12** with phenyl-terminated edge.

[*] Reinhard Berger, Prince Ravat, Dr. Manfred Wagner, Prof. Dr. Xinliang Feng, Prof. Dr. Klaus Müllen
Max-Planck-Institut für Polymerforschung
Ackermannweg 10, 55128 Mainz (Germany)
Fax: (+)49 6131 379-100
E-mail: feng@mpip-mainz.mpg.de; muellen@mpip-mainz.mpg.de
Angelos Giannakopoulos, Dr. David Beljonne
Chimie des Matériaux Nouveaux & Centre d'Innovation et de Recherche en Matériaux Polymères, Université de Mons-UMONS/Materia Nova
Place du Parc 20, B-7000 Mons (Belgium)
Fax: (+)32 (0) 65 373861
E-mail: david.beljonne@umons.ac.be

[**] We acknowledge support by the EC under the Graphene Flagship (contract no. CNECT-ICT-604391). We thank Dr. Schollmeyer , University of Mainz, for X-ray crystal structure analysis. R.B. thanks the Fond der Chemischen Industrie for a Chemiefonds fellowship. A.G acknowledges funding from the 7th Marie Curie ITN GENIUS program and the OPTI2MAT Excellence Program of Région Wallonne and FNRS/FRFC. D.B. is a research director of the Fonds National de la Recherche Scientifique-FNRS.

Supporting information for this article is available on the WWW under http://dx.doi.org/10.1002/anie.201xxxxxx.

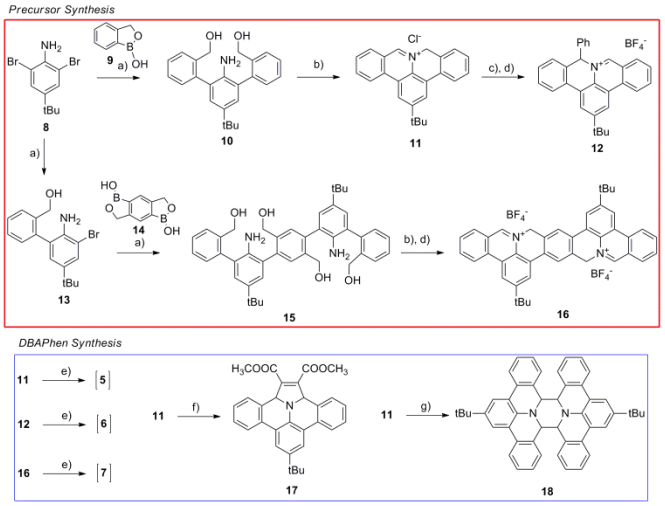

Scheme 1. Synthesis of precursors **11**, **12** and **16** and in-situ generation of DBAPhens **5** - **7**; trapping of **5** by either [3+2] cycloaddition reaction in presence of dimethoxy acetylene dicarboxylate (DMAD) to **17**, or by dimerisation to **18**. (a) $Pd(PPh_3)_4$, K_2CO_3 (2M), toluene, ethanol; b) HCl in dioxane (4M), microwave, O_2, 99%; c) PhMgBr, THF, 0 °C; d) Trityl BF_4, toluene, acetonitrile, 90 °C; e) TEA; f) DMAD, TEA, DCM, 25 °C, 53%; g) DMSO, NBu_3, 190 °C, 51%.

Although cyclisation of **10** was conducted in the presence of oxygen under harsh conditions (HCl, 130 °C, 6 bar), no decomposition by oxidation or polymerization was observed and **11** was obtained by precipitation in 99% yield. Selective α-addition of phenyl magnesium bromide to **11** and hydride abstraction at 90 °C by trityl tetrafluoroborate resulted in the kinetically controlled Hofmann-product **12** with the phenyl-substituent on the saturated α-carbon (Supporting Information, Figure S2). The stable, charged precursors **11**, **12**, and **16** are readily soluble in polar organic solvents and thus can be purified by repeated precipitation in hexane. Finally, proton abstraction reactions were performed for the resulting precursors **11, 12,** and **16** by using anhydrous triethylamine (TEA) to generate solutions of **5** – **7** under inert conditions.

As **5** – **7** could not be isolated due to their high reactivity, a solution of **5** was prepared and trapped by the presence of DMAD to afford dimethyl-8-(*tert*-butyl)-2a,13b-dihydrobenzo[7,8]indolizino[6,5,4,3-def]phenanthridine-1,2-dicarboxylate (**17**) resulting from a [3+2] cycloaddition. Interestingly, in the absence of the trapping reagent DMAD, work-up of the resulting mixture gave the dimerised compound **18** in 3% yield. Such a dimerization reaction actually has been also observed for other AMYs.[14] By preheating solutions of precursor **11** prior to the addition of tributyl amine as a high boiling base, **18** was obtained in 51% yield at 190 °C. All intermediates and precursor compounds were analyzed by ^{1}H-, ^{13}C-NMR-spectroscopy as well as HR-ESI mass spectroscopy. ^{1}H-NMR of in-situ prepared solutions of **6** showed complete conversion of the precursor **12** by, for example, the disappearance of the characteristic iminium proton at δ = 10.3 ppm. A resolved spectrum could not be obtained even if the sample was prepared and measured at -60 °C. Nevertheless, the appearance of signals in ^{1}H-NMR spectrum strongly suggests the zwitterionic structure of **6** (Supporting Information, Figure S6). The majority of AMYs cannot be characterized by ^{1}H-NMR due to their high reactivity and only few isolable AMYs were reported in literature.[15] Single crystals of the cycloadduct **17** were grown by slow evaporation of solutions in dichloromethane whose structure (Figure 2) clearly reveals the selective addition to the 1,3-positions of the AMY site. Moreover, the structure of the dimer **18** was confirmed by NMR-spectroscopy and HR-ESI.

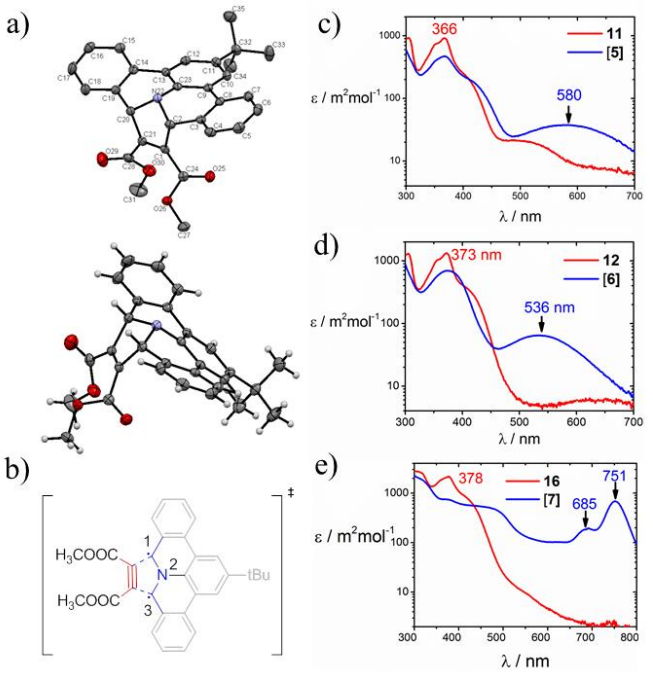

Figure 2. a) Crystal structure of cycloaddition product **17** showing selective 1,3-addition to the nitrogen side; b) proposed transient state of [2+3] cycloaddition reaction between DBAPhen **5** and DMAD; c) – e) UV-vis absorption of precursors **11**, **12**, **16** and in-situ generated solutions of DBAPhens **5**, **6**, **7** in DCM immediately after addition of base.

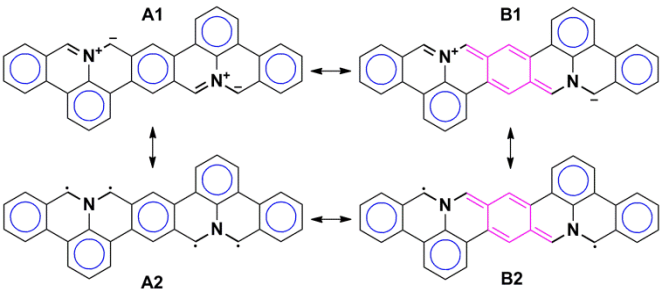

Scheme 2. Quinoid resonance stabilization between two adjacent repeating units represented in **B1** and **B2** compared to **A1** and **A2** which possess the higher number of Clar sextets (blue). In contrast to the closed-shell structure of **A1, B2** is a diradical indicating a stabilized open-shell state.

UV-vis absorption spectra of **5** – **7** were recorded in-situ under inert condition (Figure 2c). Upon generation of **5** and **6**, broad absorptions at 580 nm (536 nm) arise, which demonstrate the extended conjugation compared to their precursors **11** and **12** with maxima at 366 nm (378 nm). In contrast to **5**, the absorption of **6** is narrower and hypsochromically shifted, which supports a localization of the negative charge on the phenyl substituted carbon atom. Formation of **18** causes an absorption shoulder at 420 nm by dimerization of **5**. Similar observation is not found for the phenyl-derivative **6**. For dimer **7**, an absorption maximum at 751 nm is observed (for comparison: heptacene 728 nm),[15] with a large bathochromic shift of **7** compared to **5** – **6**, which stems from the

extended conjugation in the two mesomeric structures **A1** and **A2** (Scheme 2)**,** but also by an additional quinoid resonance stabilization of the two nitrogen centers in **B1** and **B2**.

We have used density functional theory (DFT) with the hybrid functional HSEH1PBE and the 6-31G(d) basis set to investigate the evolution of geometric and electronic structures upon oligomerisation of monomer (**5**) to tetramer (**ttm**) (Figure 3a) in the singlet (triplet) state. Besides, the lowest singlet electronic excited states and the linear optical absorption spectra of the oligomers were computed at the TD-DFT and AM1/CIS levels. An HSEH1PBE ESP charge analysis yields large positive charges of ~0.35 |e| on the nitrogen atoms and negative charges of ~-0.23 |e| on the neighboring CH units (Supporting Information, Figure S8), consistent with a sizeable ionic contribution in the ground state. In addition, the nitrogen-carbon bond lengths of ~1.36 Å indicate a close to double bond character in line with the zwitterionic **A1** form in Scheme 2. The equilibrium geometry suggests a predominant Clar formula with aromatic sextets delocalized in a zigzag orientation with respect to the longitudinal axis of the molecules, exemplified for **tm** in Figure 3b. This is borne out by the bonding-antibonding pattern in the HOMO (Figure 3c, left). Notice in particular the clear aromatic character of the benzene rings connecting the nitrogen-doped units and the presence on the carbon sites adjacent to the nitrogen atoms of localized contributions to the HOMO wave functions. There is a one-to-one correspondence between the electronic density in the HOMO and the radical form A2 (Scheme 2). Likewise, the excess spin density in the triplet state shows dominant contributions at the ribbon edges with large weights on the carbons bonded to the nitrogens, shown for **tm** (Figure 3d).

Altogether, we can conclude that the ground-state structure for the representative oligomers **7** to **ttm** can be accounted for by the superimposition of the ionic and radical aromatic Clar's formulas A1 and A2 (Scheme 2). Note also that: (i) the shape of the LUMO orbital of **ttm** (Figure 3c, right), with a quinoidic pattern on the connecting benzene rings is more consistent with Clar's formulas B1 and B2; and that (ii) the ground state of all representative molecules investigated is singlet, though the singlet-triplet energy spacing reduces from ~1 eV in the monomer **5** to ~0.2 eV in the tetramer (**ttm**). This is in agreement with the EPR result of **6** at concentration of 10^{-4} $moll^{-1}$ which did not show any signal.

The UV-Vis spectra of **5**, **7,** and **tm** have been computed at the TD-DFT and AM1/CIS levels (Supporting Information, Figures S19-S21). For the monomer **5**, both methods indicate two main absorption bands in the low-energy spectral domain, with the lowest electronic transition carrying much smaller oscillator strength. Based on their relative intensity and energetic position, we assign these two bands to the features measured at ~380 and ~540 nm in Figure 2c. As the molecular backbone gets longer (in **tm**), the lowest optical transition acquires a dominant HOMO-LUMO character, which translates into a large bathochromic and hyperchromic shift (Supporting Information, Figure S21). Both TD-DFT and AM1/CIS predict a large reduction in the optical gap as the ribbons get longer, in line with the experimental results.

Based on these findings, it is useful to extrapolate the data obtained for the oligomers **7** - **ttm** to the corresponding infinite ribbon **N-ZGNR** (Figure 4a). A linear fit to the HOMO-LUMO gap as a function of inverse length yields a ~0.23 eV bandgap. This is in good agreement with spin-polarized DFT electronic band structure calculations providing a bandgap of ~0.26eV, Figure 4e. The frontier HOCO and LUCO crystal orbitals show a large dispersion, at odds with the typical flat bands associated with edge states in zigzag ribbons. The comparison with the pristine **ZGNR** is further shown in the Supporting Information (Figures S15-S18).

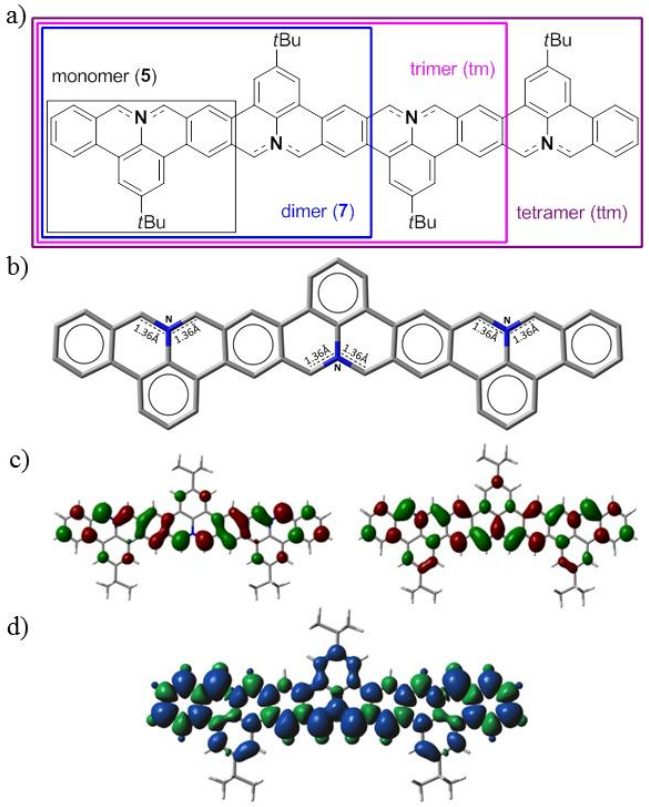

Figure 3. a) Chemical structures of trimer (**tm**) and tetramer (**ttm**). b) Equilibrium geometry of **tm**. Nitrogen-Carbon bond lengths indicate a close to double bond character in line with the A1 form (scheme 2). c) Molecular orbitals of **tm**. Left: HOMO; right: LUMO. d) spin density plot of the triplet state of **tm**.

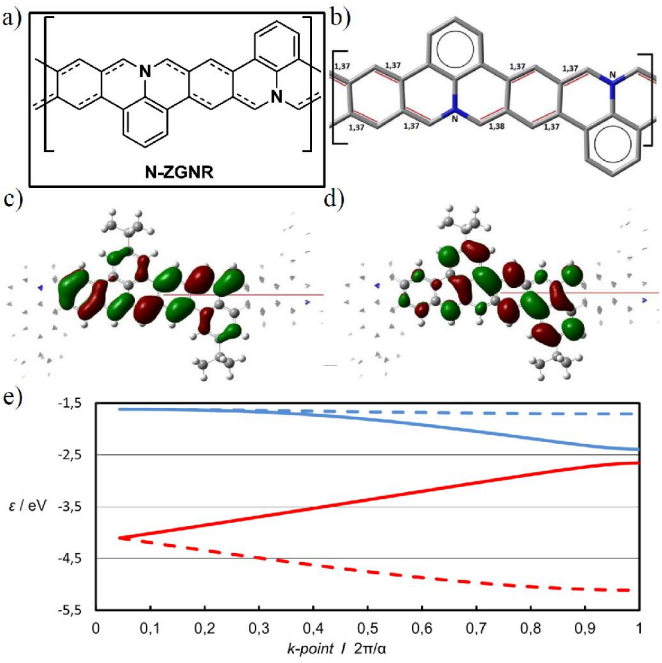

Figure 4. a) Chemical structure and b) equilibrium geometry of infinite ribbon **N-ZGNR**. Bond lengths are in line with the quinoid structures B1 and B2 (scheme 2). c),d) Molecular orbitals of **N-ZGNR** at the end of the valence and conduction band respectively (k = 2π/α). Left: HOCO; right: LUCO. e) Band structure of **N-ZGNR**.

Frontier bands are shown: HOCO-1 (dotted red), HOCO (red), LUCO (blue) and LUCO+1 (dotted blue). The unit cell of the infinite ribbon is also shown..

In summary, a bottom-up approach towards nitrogen-doped zigzag-GNRs was introduced on basis of the synthetic protocol of unprecedented DBAPhen **5**. Key-step is the deprotonation of a stable, soluble precursor **10**, which allows formation of the sensitive zigzag edge in **5** under mild and inert conditions. The possibility of lateral extension towards nitrogen-doped zigzag-GNRs was demonstrated by the synthesis of its dimer **7**. The repetition of the structural motif leads to a strong bathochromic and hyperchromic shift. DFT calculations predict the evolution of the geometric and electronic properties upon oligomerisation into an infinite nitrogen doped zigzag-ribbon **N-ZGNR**. Extension towards precursor-polymers through the same synthetic protocol is straightforward and further stabilization of the nitrogen doped zigzag-periphery is currently pursued to obtain stable nitrogen-doped zigzag-GNRs by a solution approach. Importantly, the high chemical reactivity of the *9a*-azaphenalene bears the potential as a powerful building block towards the synthesis of larger nitrogen containing polycyclic aromatic hydrocarbons.

Received: ((will be filled in by the editorial staff))
Published online on ((will be filled in by the editorial staff))

Keywords: Phenalene • Graphene Nanoribbons • Azomethine Ylides • Organic Radicals • Polycyclic Aromatic Hydrocarbons

[1] a) W. Klyne, R. Robinson, *J. Chem. Soc.* **1938**, 1991-1994; b) F. Gerson, *Helv. Chim. Acta* **1966**, *49*, 1463-1467; c) P. B. Sogo, M. Nakazaki, M. Calvin, *J. Chem. Phys.* **1957**, *26*, 1343-1345; d) D. H. Reid, *Tetrahedron* **1958**, *3*, 339-352.

[2] a) G. D. O'Connor, T. P. Troy, D. A. Roberts, N. Chalyavi, B. Fückel, M. J. Crossley, K. Nauta, J. F. Stanton, T. W. Schmidt, *J. Am. Chem. Soc.* **2011**, *133*, 14554-14557; b) M. K. Cyrański, R. W. A. Havenith, M. A. Dobrowolski, B. R. Gray, T. M. Krygowski, P. W. Fowler, L. W. Jenneskens, *Chem. – Eur. J.* **2007**, *13*, 2201-2207.

[3] a) Y. Li, K.-W. Huang, Z. Sun, R. D. Webster, Z. Zeng, W. Zeng, C. Chi, K. Furukawa, J. Wu, *Chem. Sci.* **2014**; b)Y. Li, W.-K. Heng, B. S. Lee, N. Aratani, J. L. Zafra, N. Bao, R. Lee, Y. M. Sung, Z. Sun, K.-W. Huang, R. D. Webster, J. T. López Navarrete, D. Kim, A. Osuka, J. Casado, J. Ding, J. Wu, *J. Am. Chem. Soc.* **2012**, *134*, 14913-14922.

[4] a) S. Xiao, S. J. Kang, Y. Wu, S. Ahn, J. B. Kim, Y.-L. Loo, T. Siegrist, M. L. Steigerwald, H. Li, C. Nuckolls, *Chem. Sci.* **2013**, *4*, 2018-2023; b) A. Narita, X. Feng, Y. Hernandez, S. A. Jensen, M. Bonn, H. Yang, I. A. Verzhbitskiy, C. Casiraghi, M. R. Hansen, A. H. R. Koch, G. Fytas, O. Ivasenko, B. Li, K. S. Mali, T. Balandina, S. Mahesh, S. De Feyter, K. Müllen, *Nat. Chem.* **2014**, *6*, 126-132; c) C.-A. Palma, K. Diller, R. Berger, A. Welle, J. Björk, J. L. Cabellos, D. J. Mowbray, A. C. Papageorgiou, N. P. Ivleva, S. Matich, E. Margapoti, R. Niessner, B. Menges, J. Reichert, X. Feng, H. J. Räder, F. Klappenberger, A. Rubio, K. Müllen, J. V. Barth, *J. Am. Chem. Soc.* **2014**; d) F. Schlütter, T. Nishiuchi, V. Enkelmann, K. Müllen, *Angew. Chem. Int. Ed.* **2014**, *53*, 1538-1542; e) F. Schlütter, T. Nishiuchi, V. Enkelmann, K. Müllen, *Angew. Chem.* **2014**, *126*, 1564-1568; f) X. Yang, X. Dou, A. Rouhanipour, L. Zhi, H. J. Räder, K. Müllen, *J. Am. Chem. Soc.* **2008**, *130*, 4216-4217; g) M. G. Schwab, A. Narita, Y. Hernandez, T. Balandina, K. S. Mali, S. De Feyter, X. Feng, K. Müllen, *J.Am. Chem. Soc.* **2012**, *134*, 18169-18172; h) L. Dössel, L. Gherghel, X. Feng, K. Müllen, *Angew. Chem. Int. Ed.* **2011**, *50*, 2540-2543; i) L. Dössel, L. Gherghel, X. Feng, K. Müllen, *Angew. Chem.* **2011**, *123*, 2588-2591; j) L. Chen, Y. Hernandez, X. Feng, K. Müllen, *Angew. Chem. Int. Ed.* **2012**, *51*, 7640-7654; k) L. Chen, Y. Hernandez, X. Feng, K. Müllen, *Angew. Chem.* **2012**, *124*, 7758-7773.

[5] a) L. Talirz, H. Söde, J. Cai, P. Ruffieux, S. Blankenburg, R. Jafaar, R. Berger, X. Feng, K. Müllen, D. Passerone, R. Fasel, C. A. Pignedoli, *J. Am. Chem. Soc.* **2013**, *135*, 2060-2063; b) A. Konishi, Y. Hirao, K. Matsumoto, H. Kurata, R. Kishi, Y. Shigeta, M. Nakano, K. Tokunaga, K. Kamada, T. Kubo, *J. Am. Chem. Soc.* **2013**, *135*, 1430-1437; c) A. Konishi, Y. Hirao, M. Nakano, A. Shimizu, E. Botek, B. Champagne, D. Shiomi, K. Sato, T. Takui, K. Matsumoto, H. Kurata, T. Kubo, *J. Am. Chem. Soc.* **2010**, *132*, 11021-11023; dS. Banerjee, D. Bhattacharyya, *Comput. Mater. Sci.* **2008**, *44*, 41-45; e) K. Nakada, M. Fujita, G. Dresselhaus, M. S. Dresselhaus, *Physi. Rev. B: Condens Matter Mater. Phys* **1996**, *54*, 17954-17961.

[6] a) J. Ferrer, V. M. Garcia-Suarez, *J. Mat. Chem.* **2009**, *19*, 1696-1717; b) *J. Mat. Chem.* **2009**, *19*, 1670-1671; c) R. C. Haddon, *Nature* **1975**, *256*, 394-396.

[7] P. A. Koutentis, Y. Chen, Y. Cao, T. P. Best, M. E. Itkis, L. Beer, R. T. Oakley, A. W. Cordes, C. P. Brock, R. C. Haddon, *J. Am. Chem. Soc.* **2001**, *123*, 3864-3871.

[8] a) Y. Morita, S. Suzuki, K. Sato, T. Takui, *Nat. Chem.* **2011**, *3*, 197-204; b) Z. Sun, Q. Ye, C. Chi, J. Wu, *Chem. Soc. Rev.* **2012**, *41*, 7857-7889.

[9] E. Clar, G. S. Fell, M. H. Richmond, *Tetrahedron* **1960**, *9*, 96-105.

[10] a) D. Farquhar, D. Leaver, *J. Chem. Soc. D* **1969**, 24-25; b) M. J. S. Dewar, N. Trinajstic, *J. Chem. Soc. A* **1969**, 1754-1755.

[11] S. O'Brien, D. C. C. Smith, *J. Chem. Soc.* **1963**, 2907-2917.

[12] B. Braida, C. Walter, B. Engels, P. C. Hiberty, *J. Am. Chem. Soc.* **2010**, *132*, 7631-7637.

[13] J. F. Cairns, H. R. Snyder, *J. Org. Chem.* **1964**, *29*, 2810-2812.

[14] a) P. V. Guerra, V. A. Yaylayan, *J. Agric. Food Chem.* **2010**, *58*, 12523-12529; b) F. Freeman, G. Govindarajoo, *Rev. Heteroatom Chem.* **1995**, *13*, 123-147.

[15] a) E. Lopez-Calle, M. Keller, W. Eberbach, *Eur. J. Org. Chem.* **2003**, *2003*, 1438-1453; b)Y. Kobayashi, I. Kumadaki, T. Yoshida, *Heterocycles* **1977**, *8*, 387-390; c) J. P. Freeman, *Chem. Rev.* **1983**, *83*, 241-261; d) H. Seidl, R. Huisgen, R. Knorr, *Chem. Ber.* **1969**, *102*, 904-914.

Zigzag Ribbon

Reinhard Berger, Angelos Giannakopoulos, Prince Ravat, Manfred Wagner, David Beljonne, Xinliang Feng,* Klaus Müllen**____ **Page – Page**

Synthesis of Nitrogen Doped ZigZag-Edge Peripheries: Dibenzo-*9a*-azaphenalene as Repeating Unit

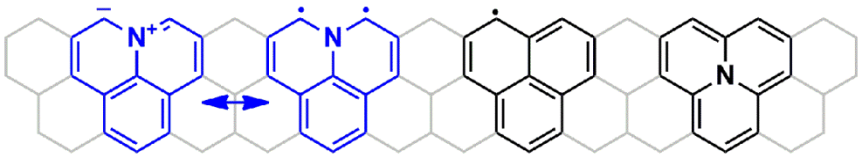

Based on unprecedented dibenzo-9*a*-azaphenalene as core motif, a bottom-up approach toward stable and monodisperse segments of graphenes with a nitrogen doped zigzag-edge is introduced targeting larger nitrogen doped zigzag-nanographenes and graphene nanoribbons.